Original Article

N-acetylcysteine, a small molecule scavenger of reactive oxygen species, alleviates cardiomyocyte damage by regulating *OPA1*-mediated mitochondrial quality control and apoptosis in response to oxidative stress

Junyi Zheng[1,2], Lili Zhao[2], Yuanyuan Liu[1,2], Mengying Chen[1,2], Xukun Guo[1,2], Jixiang Wang[1,2]

[1]Department of Cardiology, Tianjin Chest Hospital, Tianjin, China; [2]Tianjin Institute of Cardiovascular Disease, Tianjin Chest Hospital, Tianjin, China

Contributions: (I) Conception and design: J Zheng, X Guo, J Wang; (II) Administrative support: L Zhao, Y Liu, M Chen; (III) Provision of study materials or patients: L Zhao, Y Liu, M Chen; (IV) Collection and assembly of data: J Zheng, L Zhao, Y Liu, M Chen; (V) Data analysis and interpretation: J Zheng, L Zhao, Y Liu, M Chen; (VI) Manuscript writing: All authors; (VII) Final approval of manuscript: All authors.

Correspondence to: Jixiang Wang, MD; Xukun Guo, MD. Department of Cardiology, Tianjin Chest Hospital, No. 261 South Taierzhuang Road, Jinnan District, Tianjin 300222, China; Tianjin Institute of Cardiovascular Disease, Tianjin Chest Hospital, Tianjin, China. Email: 25254791@qq.com; guoxukun206@126.com.

Background: Oxidative stress-induced mitochondrial damage is the major cause of cardiomyocyte dysfunction. Therefore, the maintenance of mitochondrial function, which is regulated by mitochondrial quality control (MQC), is necessary for cardiomyocyte homeostasis. This study aimed to explore the underlying mechanisms of N-acetylcysteine (NAC) function and its relationship with MQC.

Methods: A hydrogen peroxide-induced oxidative stress model was established using H9c2 cardiomyocytes treated with or without NAC prior to oxidative stress stimulation. Autophagy with light chain 3 (LC3)-green fluorescent protein (GFP) assay, reactive oxygen species (ROS) with the 2',7'-dichlorodi hydrofluorescein diacetate (DCFH-DA) fluorescent, lactate dehydrogenase (LDH) release assay, adenosine triphosphate (ATP) content assay, and a mitochondrial membrane potential detection were used to evaluate mitochondrial dynamics in H_2O_2-treated H9c2 cardiomyocytes, with a focus on the involvement of MQC regulated by NAC. Cell apoptosis was analyzed using caspase-3 activity assay and Annexin V-fluorescein isothiocyanate (V-FITC)/propidium iodide (PI) double staining.

Results: We observed that NAC improved cell viability, reduced ROS levels, and partially restored optic atrophy 1 (OPA1) protein expression under oxidative stress. Following transfection with a specific *OPA1*-small interfering RNA, the mitophagy, mitochondrial dynamics, mitochondrial functions, and cardiomyocyte apoptosis were evaluated to further explore the mechanisms of NAC. Our results demonstrated that NAC attenuated cardiomyocyte apoptosis via the ROS/*OPA1* axis and protected against oxidative stress-induced mitochondrial damage via the regulation of *OPA1*-mediated MQC.

Conclusions: NAC ameliorated the injury to H9c2 cardiomyocytes caused by H_2O_2 by promoting the expression of *OPA1*, consequently improving mitochondrial function and decreasing apoptosis.

Keywords: N-acetylcysteine (NAC); mitochondrial quality control (MQC); optic atrophy 1 (OPA1); mitophagy; cardiomyocyte

Submitted Jun 06, 2024. Accepted for publication Jul 19, 2024. Published online Aug 21, 2024.
doi: 10.21037/jtd-24-927
View this article at: https://dx.doi.org/10.21037/jtd-24-927

Introduction

Cardiac disease, a collective term describing multiple conditions, such as hypertrophic cardiomyopathy, myocardial infarction, and ischemia-reperfusion injury, is the leading cause of death worldwide (1). Mitochondria-associated oxidative stress and energy metabolism dysregulation are common pathological processes identified in heart disease and the major causes of cardiomyocyte dysfunction (2,3). Oxidative stress is defined as excessive reactive oxygen species (ROS) production and/or decreased antioxidant capacity, leading to an imbalanced oxidative/antioxidant system. Mitochondria, which account for 30% of cardiomyocyte volume, deliver ~90% of the energy required by cardiomyocytes (4). To adapt to environmental changes, mitochondria respond to diverse stimuli via intracellular signaling, which affects cellular outcomes (5). As mitochondria are located at the major sites of ROS production and are constantly surrounded by ROS *in situ*, they are susceptible to structural and functional damage (6). Therefore, the maintenance of mitochondrial function is essential for cardiomyocyte protection during oxidative stress.

Mitochondrial function is regulated by mitochondrial dynamics and mitophagy; that is, mitochondrial quality control (MQC). To maintain their morphology, distribution, and function, mitochondria undergo continuous fusion and fission, known as mitochondrial dynamics (7,8). The regulation of mitochondrial fusion requires two key proteins, optic atrophy 1 (OPA1) and mitofusin (MFN), which are located on the inner and outer membranes of mitochondria, respectively. Conversely, mitochondrial fission depends on dynamin-related protein 1 (DRP1), which interacts with mitochondrial fission 1 protein (FIS1). Mitochondrial dynamics play an important role in cardiomyocyte function, and reduced fusion and excessive fission are associated with impaired mitochondrial function (9-11), inducing excessive ROS production and subsequent disease (12).

OPA1 is a key protein involved in the regulation of mitochondrial dynamics; it facilitates inner-membrane fusion and regulates other mitochondrial dynamics-related proteins, such as MFN, DRP1, and FIS1 (13,14). In addition, *OPA1* is involved in the organization and maintenance of mitochondrial cristae and the regulation of mitophagy (15). *OPA1* downregulation results in the inhibition of mitochondrial fusion and cristae remodeling, promoting spontaneous cytochrome c release and triggering apoptosis (16). Damaged mitochondria are recognized as a mitophagy substrate, leading to their clearance and degradation (17). This prevents the accumulation of mitochondrial DNA mutations and metabolic dysregulation (18), while enhanced mitochondrial fusion prevents the removal of defective mitochondria by mitophagy. There is increasing evidence that *OPA1* is directly linked to the mitochondrial structure and bioenergetic functions (19,20). This is particularly important for cardiac tissues, as the majority of the required energy is supplied by mitochondria. Therefore, *OPA1*-mediated mitochondrial dynamics homeostasis is a stress-sensitive cellular response that is considered the gatekeeper of mitochondrial function (21).

N-acetylcysteine (NAC) is a sulfur-containing reducing agent with cardioprotective properties. NAC decreases cardiomyocyte apoptosis by regulating the redox status of intracellular antioxidants (22), inhibiting inflammasome activation (23), removing free radicals (24), and inhibiting endoplasmic reticulum stress (25). As an ROS scavenger, NAC maintains mitochondrial function by inhibiting excessive oxidative stress; however, it is not known whether the protective role of NAC is related to MQC. Undifferentiated H9c2 cells, a commonly utilized *in vitro* cell model as a substitute for cardiomyocytes, demonstrate the capacity to differentiate into a heart-like phenotype under reduced serum concentrations of all-trans retinoic acid in the culture medium, resulting in the formation of multinucleated cells with limited proliferative potential.

Highlight box

Key findings

- Our findings indicate that N-acetylcysteine (NAC) mitigates cardiomyocyte apoptosis through the reactive oxygen species/optic atrophy 1 (ROS/*OPA1*) axis and safeguards against oxidative stress-induced mitochondrial damage by regulating *OPA1*-mediated mitochondrial quality control (MQC).

What is known, and what is new?

- Oxidative stress-induced mitochondrial damage is the major cause of cardiomyocyte dysfunction. The maintenance of mitochondrial function, which is regulated by MQC, is necessary for cardiomyocyte homeostasis.
- Our study identified a novel mechanism by which NAC mitigates cardiomyocyte injury through the regulation of MQC via ROS/*OPA1* axis in the presence of oxidative stress.

What is the implication, and what should change now?

- NAC could serve as an innovative therapeutic approach for cardiac disease. Additionally, the findings of this study provide a potential theoretical framework for subsequent research.

Undifferentiated H9c2 cells are predominantly employed in the investigation of cardiac signaling pathways due to their ease of proliferation and availability, possession of myoblastic characteristics, and ability to mimic cardiomyocyte functionality in experimental settings (26,27). Therefore, using H9c2 cardiomyocytes, we established a H_2O_2-induced oxidative stress model and investigated the underlying mechanisms of NAC. In addition, we examined the role of autophagy, ROS with the 2',7'-dichlorodi hydrofluorescein diacetate (DCFH-DA) fluorescent, lactate dehydrogenase (LDH) release assay, adenosine triphosphate (ATP) content assay, and a mitochondrial membrane potential detection in modulating mitochondrial dynamics in H_2O_2-treated H9c2 cardiomyocytes, with a focus on the involvement of MQC regulated by NAC. We present this article in accordance with the MDAR reporting checklist (available at https://jtd.amegroups.com/article/view/10.21037/jtd-24-927/rc).

Methods

Cell culture

H9c2 cells (Catalogue number: 1101RAT-PUMC000219; The Cell Resource Center, Peking Union Medical College, Beijing, China) were cultured in Dulbecco's modified Eagle medium (DMEM) containing 10% fetal bovine serum and 1% penicillin-streptomycin (Thermo Fisher Scientific, Waltham, MA, USA). The cells were kept in an incubator of humidified 5% carbon dioxide at 37 ℃ and subcultured every 2–3 days. The cells in the H_2O_2 group were treated with 25–1,000 μmol/L of H_2O_2 for 12 h, or 250 μmol/L of H_2O_2 for 3, 6, 12, or 24 h. The cells in the NAC group were pretreated with 1 mmol/L of NAC (Catalogue number: 38520-57-9; Merck, Darmstadt, Germany) for 1 h prior to oxidative stress stimulation. Each experiment was biologically repeated three times. Cells from the second and third generations are utilized in cell experimental studies.

Cell viability assay

Cell viability was evaluated using the Cell Counting Kit-8 (Catalogue number: CK04; CCK8, Dojindo Laboratories, Kumamoto, Japan) following the manufacturer's protocol.

Cellular ROS assay

Cellular ROS were detected using an ROS assay kit (Catalogue number: S0033M; Beyotime, Shanghai, China). Briefly, the DCFH-DA fluorescent probe was diluted in DMEM to a final concentration of 10 μmol/L. After H_2O_2 treatment, the cells were trypsinized and collected using centrifugation. The 50 μL of diluted DCFH-DA solution was added, and the cells were incubated with the probe at 37 ℃ for 20 min. The cells were mixed every 3–5 min to ensure the equal distribution of the probe during incubation. Next, the cells were washed three times with DMEM, and cellular ROS were detected using flow cytometry (BD FACSCelesta™, Bergen County, NJ, USA).

Cell transfection

The cells were cultured in a 6-well plate until ~70% confluence was reached. Next, the cell culture medium was replaced, and the cells were transfected with *OPA1*-small interfering (siRNA) or scramble control siRNA using Lipofectamine 3000 (Thermo Fisher, USA) according to the manufacturer's instructions. Furthermore, real-time quantitative polymerase chain reaction (RT-qPCR) was employed to confirm the transfection efficiency of siRNA. A transfection rate was deemed satisfactory when the silencing efficiency of the target gene reached 80% or higher, prompting the continuation of subsequent cell experiments.

Western blot

Western blot was performed as described previously (28). The following primary antibodies were used to incubate the membranes: anti-Cytochrome C (Cat No: 66264-1-Ig; dilution: 1:1,000, Proteintech, Rosemont, IL, USA), anti-voltage-dependent anion channel (VDAC) (Cat No: 66345-1-Ig; dilution: 1:1,000, Proteintech), or anti-glyceraldehyde-3-phosphate dehydrogenase (GAPDH) (Cat No: 60004-1-Ig; dilution: 1:10,000, Proteintech) at 4 ℃ overnight. After washing three times with phosphate buffered saline with Tween 20 (PBST), the membranes were incubated with a secondary antibody (Cat No: RGAM001; dilution: 1:10,000, Proteintech) for 1 h. Immunoblots were developed and analyzed using a gel imaging system (Vilber Lourmat, France).

RT-qPCR

According to the manufacturer's instructions, a commercial TRIzol reagent (Thermo Fisher, USA) was used to extract the total RNA from the cells. The total RNA (2 μg) was

Table 1 A list of the primers used for RT-qPCR

Primer	Sequence (5' to 3')
R-GAPDH forward	AACTCCCATTCTTCCACC
R-GAPDH reverse	ACCACCCTGTTGCTGTAG
R-Fis1 forward	ACTTCTTCTACCCGGAGGCT
R-Fis1 reverse	CTCTACAGGCACTTTGGGGG
R-Drp1 forward	TGGAAAGAGCTCAGTGCTGG
R-Drp1 reverse	ACTCCATTTTCTTCTCCTGTTGT
R-Mfn1 forward	CAAACTGCAGCCACCAAGTC
R-Mfn1 reverse	CTCGGGTGGAGAAACTGCTT
R-Mfn2 forward	ACCAGCTAGAAACGAGATGTCC
R-Mfn2 reverse	GTGCTTGAGAGGGGAAGCAT
R-Opa1 forward	ATTTCGCTCCTGACCTGGAC
R-Opa1 reverse	GGTGTACCCGCAGTGAAGAA

RT-qPCR, real-time quantitative polymerase chain reaction.

reverse-transcribed into complementary DNA using a reverse-transcription system (Promega, Madison, WI, USA). The RT-qPCR method was used to measure the messenger RNA (mRNA) level of the target genes *OPA1*, mitofusin 1 (*MFN1*), mitofusin 1 (*MFN2*), fission protein 1 (*FIS1*), and glyceraldehyde-3-phosphate dehydrogenase (*GAPDH*) with the SYBR Green qPCR kit (Roche, Basel, Switzerland). The primers were synthetized by Sangon Biotech Co., Ltd., Shanghai, China as shown in *Table 1*.

Autophagy and mitochondria imaging

MQC denotes the cellular process through which structural and functional integrity of mitochondria is upheld via diverse mechanisms aimed at preserving cellular homeostasis. These mechanisms encompass mitochondrial fusion, division, autophagy, mitophagy, and protease-mediated degradation (29). In our study, we examined the role of autophagy in modulating mitochondrial dynamics in H_2O_2-treated H9c2 cardiomyocytes, with a focus on the involvement of MQC regulated by NAC. Light chain 3 (LC3)-green fluorescent protein (GFP) plasmids and a mitochondrion-selective Mito-dsRed (Hanbio, China) were used to visualize autophagosomes and mitochondria, respectively. The cells were cultured in imaging dishes (NEST, Wuxi, Jiangsu, China) for 12 h, transfected with the LC3-GFP plasmids, and then incubated for 8 h. Next, the culture medium was changed, Mito-dsRed was added to the medium, and the cells were incubated for 48 h before the H_2O_2 treatment. The cells were then washed with phosphate buffered saline (PBS), fixed with 4% paraformaldehyde (Thermo Fisher, USA) and stained with 4',6-diamidino-2-phenylindole (DAPI). Autophagosomes and mitochondria were observed using a laser-scanning confocal microscope (Zeiss, Germany).

Mitochondria isolation

Mitochondria were isolated using a reagent-based method according to the manufacturer's instructions (Thermo Fisher, USA). Briefly, the cells were pelleted by centrifugation at 850 ×g for 2 min and then lysed in reagents A, B, and C as indicated in the protocol. Next, the pellets were centrifuged at 700 ×g for 10 min at 4 ℃, the supernatant was transferred to a new tube, and then centrifuged at 12,000 ×g for 15 min at 4 ℃. Finally, the supernatant containing the cytosol fraction was transferred to a new tube on ice, 500 µL of reagent C was added to the pellets, the samples were centrifuged at 12,000 ×g for 5 min, and the isolated mitochondria (precipitate) were then collected.

Apoptosis assay

The apoptosis rate was detected using an Annexin V-fluorescein isothiocyanate (V-FITC)/propidium iodide (PI) cell apoptosis detection kit (Catalogue number: WLA001a; Wanleibio, Shenyang, China). Briefly, the cells were trypsinized and then centrifuged at 800 rpm for 5 min. The cells were washed twice with PBS, and then resuspended in 500 µL of binding buffer and stained with 5 µL of Annexin V-FITC and 5 µL of PI at room temperature for 10 min in the dark. The apoptosis rate was then detected using a flow cytometer (BD FACSCelesta™, Bergen County, NJ, USA).

Caspase-3 activity assay

Caspase-3 activity was determined using a caspase-3 activity assay kit (Catalogue number: C1073M; Beyotime, China). Briefly, the cells were trypsinized, resuspended in cell culture medium, and the cell precipitate was then obtained via centrifugation at 600 ×g and 4 ℃ for 5 min. Lysis buffer (100 µL) was added to the cell precipitate and thoroughly mixed. The samples were incubated at 4 ℃ for 15 min, centrifuged at 20,000 ×g for 15 min at 4 ℃, and caspase-3 activity was detected in the supernatant as described in the

manufacturer's protocol.

Mitochondrial membrane potential (the Supernatant)

A mitochondrial membrane potential detection kit (JC-1) (Catalogue number: C2003S; Beyotime, China) was used to measure ΔΨm according to the manufacturer's protocol. Briefly, the culture medium was removed, and the cells were washed with PBS. Equal volumes of fresh culture medium and JC-1 dye were added to the cells, mixed, and incubated at 37 ℃ for 20 min. The cells were then washed three times with the washing buffer, 2 mL of fresh culture medium was added, and ΔΨm was detected using a laser-scanning confocal microscope (Zeiss, Germany).

ATP content assay

ATP content was detected using an ATP detection kit (Solarbio, China) according to the manufacturer's protocol. Briefly, 400 µL of lysis buffer was added to each well and pipetted repeatedly to ensure full lysis. The lysates were centrifuged at 10,000 ×g for 10 min at 4 ℃. The supernatants were collected, 500 µL chlorine was added, and the samples were then thoroughly mixed, and centrifuged at 10,000 ×g at 4 ℃ for 3 min. Next, the supernatants were transferred to another tube on ice, thoroughly mixed with a test reagent and working solution, and the absorbance of the samples at 340 nm was detected after 10 s. The cuvette with the reaction solution was then placed in a 37 ℃ water bath for 3 min, and the absorbance was detected again at 3 min 10 s. The ATP content of the samples was calculated according to the manufacturer's protocol.

LDH release assay

LDH release was measured using a commercial LDH detection kit (Catalogue number: C0016; Beyotime, China). Briefly, the cells were washed with PBS and the culture medium was replaced before the experiment. The background blank control group and maximum enzyme activity control group were established. One hour before the scheduled detection time point, 10% of the original culture medium volume of LDH release reagent was added to the "maximum enzyme activity control group" and incubated for 1 h in the 37 ℃ cell incubator. Next, a solution consisting of 120 µL of supernatant from each group and 60 µL of work solution was mixed gently at 25 ℃ for 30 min on a shaker (in the dark), and the absorbance at 490 nm was measured using a multimode microplate reader (Molecular Devices, Sunnyvale, CA, USA).

Statistical analysis

The data were analyzed using the SPSS statistical software (version 22, IBM SPSS Statistics, Chicago, IL, USA), and are expressed as the mean ± standard deviation (SD). A one-way analysis of variance (ANOVA) was used for the multiple-group comparisons, and the least significant difference post-hoc test was used for the intergroup comparisons. All the experiments were performed independently in triplicate. Statistical significance was set at $P<0.05$.

Results

NAC increased cell viability and reduced ROS content in response to oxidative stress

H_2O_2 is a well-characterized reagent used to induce oxidative stress; it induces either apoptosis or necrosis, depending on the treatment concentration and duration (30). First, we performed cell viability experiments by incubating H9c2 with 25–1,000 µmol/L of H_2O_2 for 24 h, and our results showed that cell viability gradually decreased as H_2O_2 concentration increased in a dose-dependent manner (*Figure 1A*). Next, we performed time-course experiments using a H_2O_2 concentration of 250 µmol/L. Based on the results of these experiments (*Figure 1B*), 250 µmol/L of H_2O_2 and a 12-h duration were selected as the optimal conditions for inducing oxidative damage. To explore the cardioprotective properties of NAC, we treated the H9c2 cells with H_2O_2 in the absence or presence of NAC. Our results showed that H_2O_2 decreased cell viability by ~40% (*Figure 1C*) and nearly doubled the intracellular ROS content, while these effects were partially reversed by NAC (*Figure 1D,1E*).

NAC affects OPA1-mediated mitophagy

Mitophagy is the main mechanism of MQC (29), and *OPA1*-mediated mitophagy is involved in oxidative stress (31). To understand the effects of NAC on the cardiomyocyte MQC response to oxidative stress injury, we evaluated the effect of *OPA1* silencing on the cardioprotective properties of NAC. The RT-qPCR results showed that compared with the control cells, H_2O_2 treatment impaired *OPA1* transcription. The addition of NAC restored the *OPA1* level, and this

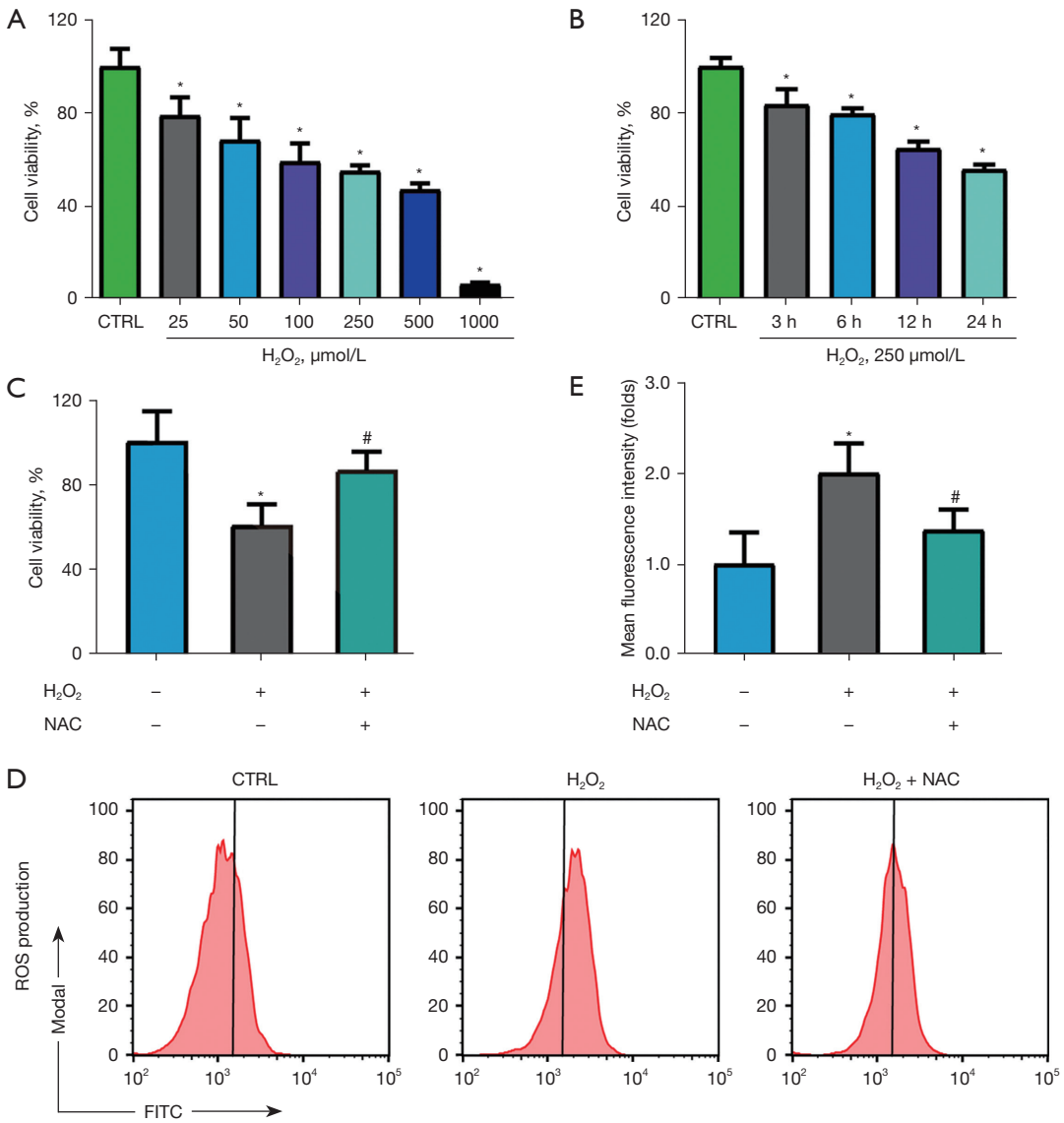

Figure 1 NAC reduces ROS content in response to oxidative stress. (A) Cell viability of H9c2 cardiomyocytes incubated with 25–1,000 μmol/L of H_2O_2 for 24 h. (B) Cell viability of H9c2 cardiomyocytes incubated with 250 μmol/L of H_2O_2 for different periods. (C-E) H9c2 cardiomyocytes were treated with 250 μmol/L of H_2O_2 for 12 h with or without 1 mmol/L NAC pretreatment, and cell viability (C) and ROS production (D,E) were measured by flow cytometer. Statistical comparisons were performed using a one-way ANOVA. *, P<0.05 *vs.* control group; #, P<0.05 *vs.* H_2O_2 group. CTRL, control; NAC, N-acetylcysteine; ROS, reactive oxygen species; FITC, fluorescein isothiocyanate; ANOVA, analysis of variance.

effect was inhibited by *OPA1* downregulation (*Figure 2A*). To intuitively explore the effect of NAC on *OPA1*-mediated mitophagy, we transfected the H9c2 cells with LC3-GFP plasmids and Mito-dsRed. The H_2O_2 treatment increased the number of autophagosomes that co-localized with mitochondria, which was weaker in the NAC condition. However, *OPA1* knockdown restored the activation of mitophagy (*Figure 2B,2C*).

Silencing of OPA1 inhibits mitochondrial dynamics regulated by NAC

Mitochondria are dynamic organelles that constantly change shape to adapt to the environment. The balance

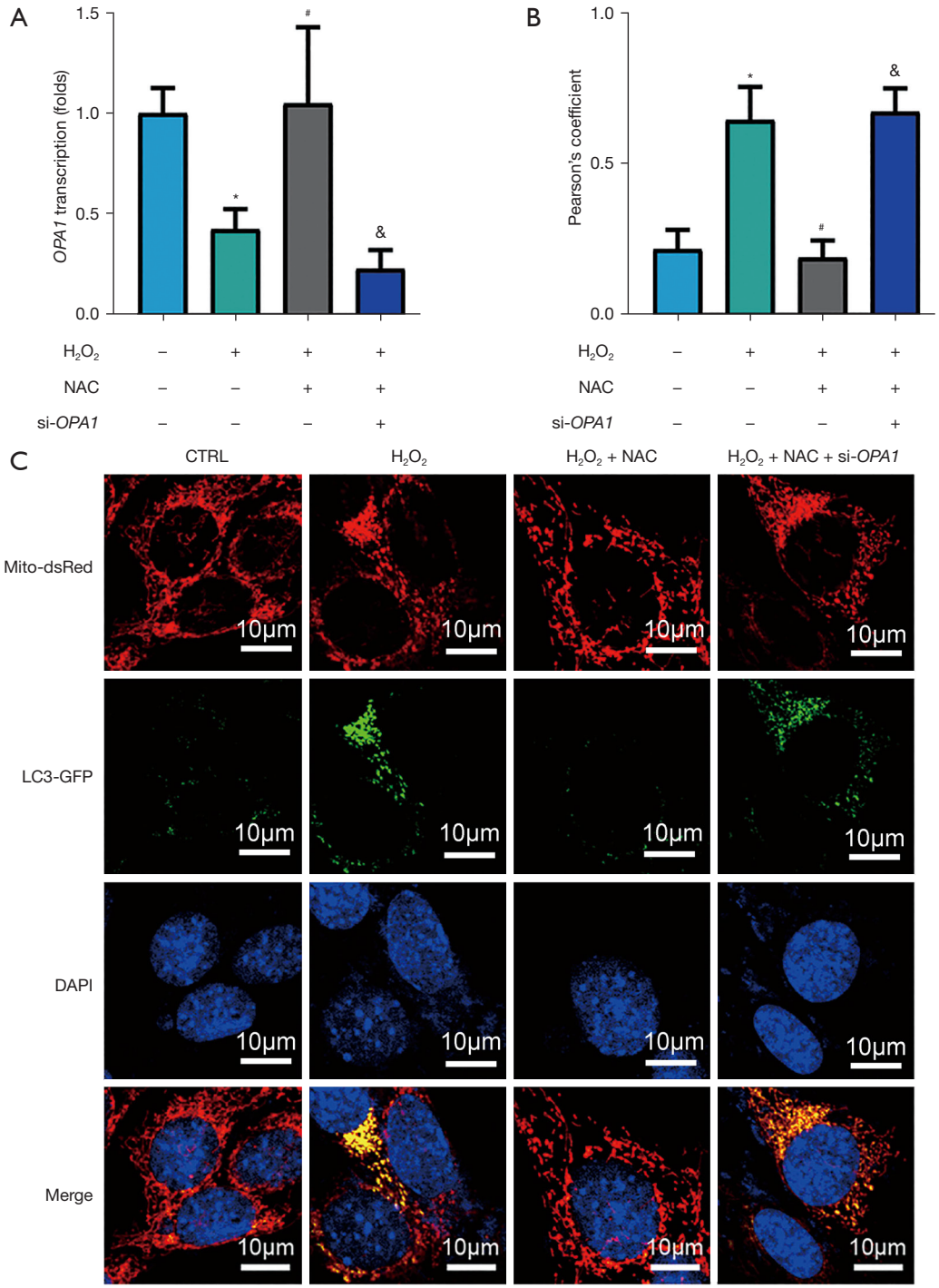

Figure 2 NAC regulates H9c2 cardiomyocyte mitophagy via *OPA1*. H9c2 cardiomyocytes were transfected with *OPA1*-siRNA, and (A) the *OPA1* transcription level was detected using RT-qPCR and normalized to GAPDH. (B) Graph quantifying LC3 signal overlapping mitochondria in different conditions. (C) A confocal laser-scanning microscope was used to observe mitophagy. The cells transfected with LC3-GFP were stained with Mito-dsRed, and counterstained with DAPI. Scale bar =10 μm. Statistical comparisons were performed using a one-way ANOVA. *, P<0.05 *vs.* control group; #, P<0.05 *vs.* H_2O_2 group; &, P<0.05 *vs.* NAC group. CTRL, control; NAC, N-acetylcysteine; DAPI, 4,6-diamino-2-phenylindole; RT-qPCR, real-time quantitative polymerase chain reaction; GAPDH, glyceraldehyde-3-phosphate dehydrogenase; ANOVA, analysis of variance.

of mitochondrial dynamics, including fusion and fission, plays a vital role in cardiomyocyte function. Therefore, we first assessed mitochondrial morphology and found that oxidative stress decreased the number of filiform- or tubular-shaped mitochondria, but increased the number of puncta-shaped mitochondria. Further, NAC markedly reduced the effect of H_2O_2; however, the effect of NAC was reversed by *OPA1* silencing (*Figure 3A*). We then evaluated the mRNA level of mitochondrial dynamic markers, such as *MFN1*, *MFN2*, *DRP1*, and *FIS1*, using RT-qPCR, and the expression levels of the markers were normalized to that of *GAPDH*. The results showed that the H_2O_2 treatment decreased the transcription levels of MFN1 and MFN2 and increased those of DRP1 and FIS1. However, H_2O_2 did not affect the MFF transcription levels (data not shown). The NAC pretreatment reversed these effects, while *OPA1* knockdown inhibited NAC-induced changes in the levels of mitochondrial dynamics markers (*Figure 3B-3E*).

NAC inhibited cardiomyocyte apoptosis via OPA1

A close relationship has been established between mitochondrial dynamics, mitophagy, and apoptosis, as the regulation of mitochondrial dynamics and mitophagy can alleviate apoptosis. Cytochrome c is normally located in the mitochondrial cristae and regulated by *OPA1*, and its release from mitochondria into the cytoplasm is considered the main intracellular trigger of apoptosis. Therefore, we first evaluated the localization of cytochrome c by western blot. The H_2O_2 treatment decreased the mitochondrial cytochrome c levels and increased the cytoplasmic levels, which confirmed the release of cytochrome c. Conversely, NAC significantly reduced this effect. Further, *OPA1* knockdown reversed the effect of NAC on cytochrome c release (*Figure 4A-4C*). Next, flow cytometry experiments of H9c2 cardiomyocytes double stained with Annexin V-FITC and PI-PE were used to measure the apoptosis rate. As *Figure 4D*,*4E* show, the H_2O_2 treatment increased the apoptosis rate compared to that of the control cells, and the NAC treatment reduced the apoptosis rate. The apoptosis rate of the *OPA1* silencing cells was dramatically increased. The pattern of activity for caspase-3 was consistent with the apoptosis rate observed by the flow cytometry experiments (*Figure 4F*).

NAC preserved mitochondrial function through OPA1

Next, we examined the effect of NAC on mitochondrial function and its connection to *OPA1*. A JC-1 probe was used to measure ΔΨm in the H9c2 cardiomyocytes treated with H_2O_2 with or without NAC pretreatment. Our results showed that the H_2O_2 treatment increased the levels of monomeric JC-1 (with green indicating depolarization), while NAC reduced the monomeric JC-1 levels; however, these changes were reversed by *OPA1* silencing (*Figure 5A*,*5B*). The ATP content and LDH production were measured to evaluate mitochondrial function; H_2O_2 suppressed the intracellular ATP content and induced LDH release, which were reversed upon NAC pretreatment, while *OPA1* knockdown inhibited the NAC-mediated effects (*Figure 5C*,*5D*).

Discussion

In this study, we explored the protective effects of NAC and its role in MQC using a H_2O_2-induced oxidative stress model. NAC suppressed ROS, increased *OPA1* protein expression levels, and contributed to the recovery of mitochondrial morphology. Our findings clarified the mechanism of NAC action on restored mitochondrial functions and decreased myocardial apoptosis via *OPA1*-mediated mitochondrial dynamics and mitophagy.

H_2O_2 is a well-characterized reagent used to induce oxidative stress. Wang *et al.* (32) reported that 100 μmol/L of H_2O_2 induced H9c2 cell apoptosis in a time-dependent manner, while 500 μmol/L of H_2O_2 treatment caused necrosis. In this study, our results demonstrated that the ROS content and apoptosis rate increased exposure to H_2O_2 with a concentration of 250 μmol/L. ROS perform seemingly contradictory functions depending on their levels (33): at low concentrations, ROS regulate signal transduction pathways and participate in cell growth, differentiation, and apoptosis, while excessive ROS accumulation leads to oxidative damage, causing mitochondrial dysfunction, DNA mutations, protein oxidation, and membrane lipid peroxidation. Lin *et al.* reported that NAC suppressed apoptotic signal kinase 1 phosphorylation and regulated the redox status of intracellular antioxidant proteins to decrease apoptosis (34). Similarly, we also observed that NAC reduced apoptosis, even though we used a H_2O_2 concentration of 250 μmol/L rather than the concentration of 750 μmol/L that Lin *et al.* used in their experiments (34).

In eukaryotic cells, mitochondria exist as a reticular network that is dynamically regulated by fusion and fission. A disruption of mitochondrial dynamics in myocardial

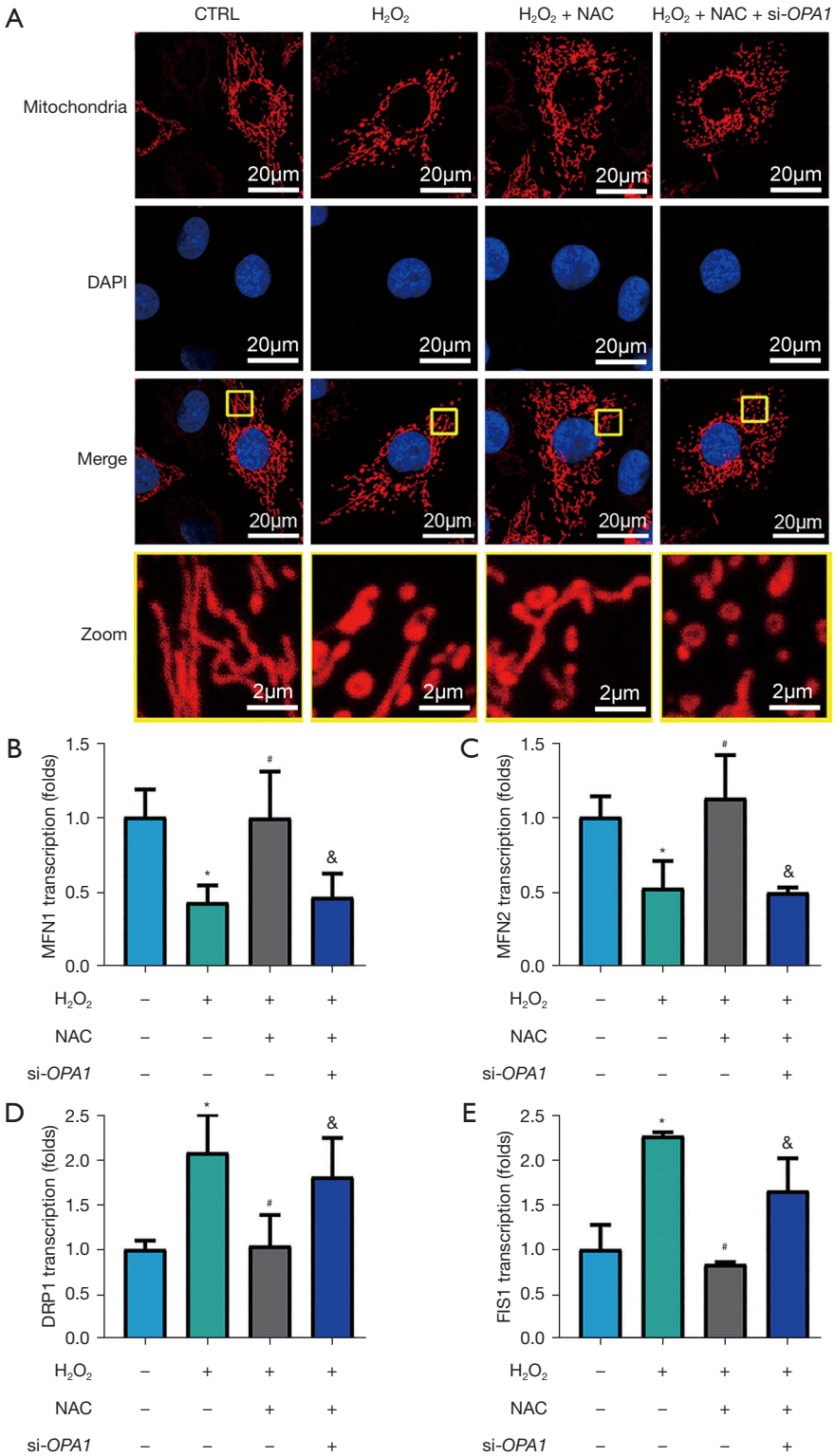

Figure 3 NAC regulates mitochondrial dynamics in H9c2 cardiomyocytes via *OPA1*. (A) The cells were stained with a mitochondrion-specific Mito-dsRed probe, and the mitochondrial morphology was observed using a confocal laser-scanning microscope (scale bar =20 μm, magnification 1,600×). (B-E) H9c2 cardiomyocytes were treated with 250 μmol/L of H_2O_2 for 12 h with or without 1 mmol/L of NAC

pretreatment. The transcription levels of the mitochondrial dynamic genes *MFN1*, *MFN2*, *DRP1*, and *FIS1* were evaluated by RT-qPCR and normalized to GAPDH. Statistical comparisons were performed using a one-way ANOVA. *, P<0.05 *vs.* control group; #, P<0.05 *vs.* H_2O_2 group; &, P<0.05 *vs.* NAC group. CTRL, control; NAC, N-acetylcysteine; RT-qPCR, real-time quantitative polymerase chain reaction; GAPDH, glyceraldehyde-3-phosphate dehydrogenase; ANOVA, analysis of variance.

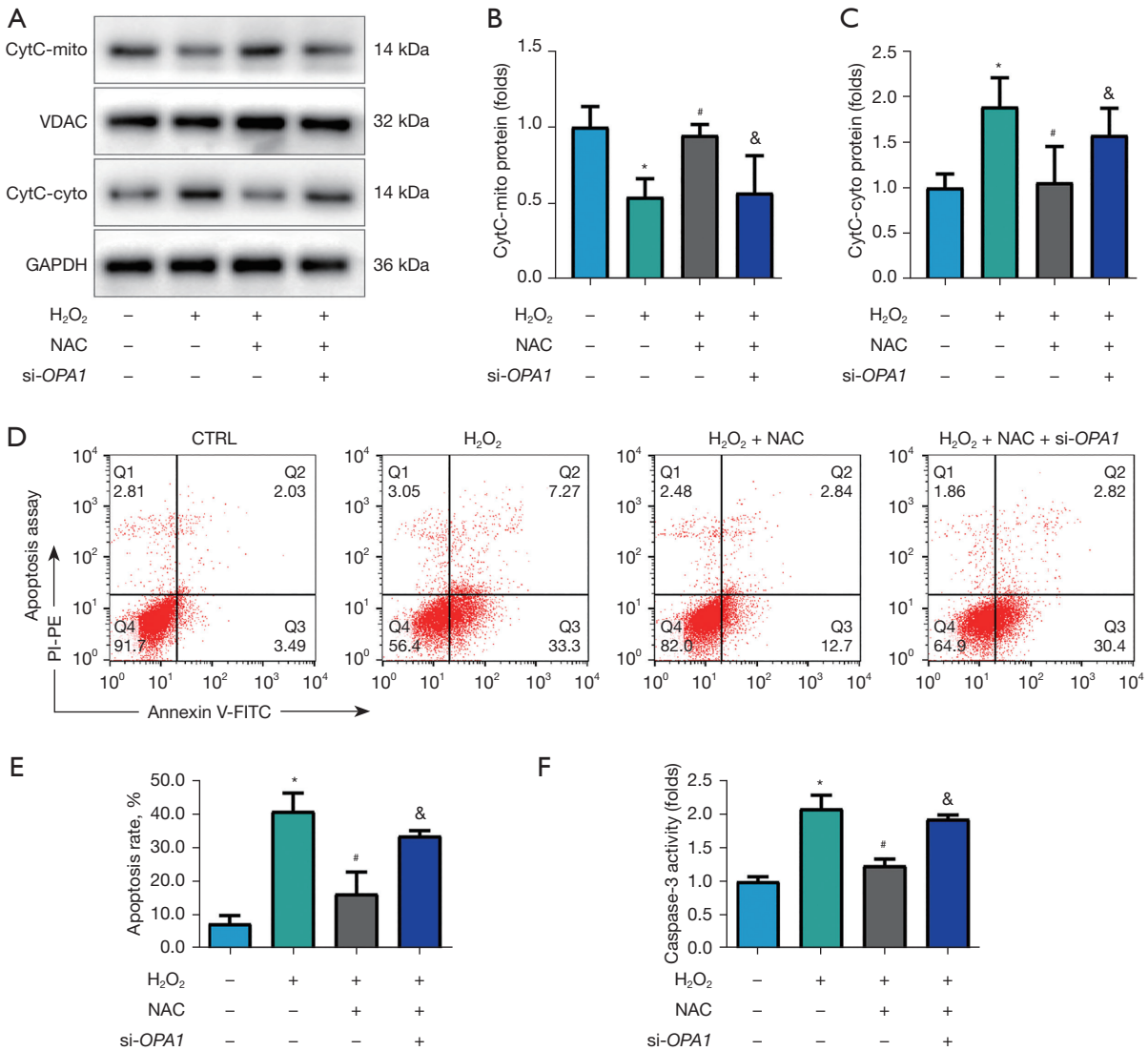

Figure 4 NAC regulates H9c2 cardiomyocyte apoptosis via *OPA1*. H9c2 cardiomyocytes were treated with 250 μmol/L of H_2O_2 for 12 h with or without 1 mmol/L of NAC pretreatment. (A-C) The release of cytochrome c from mitochondria to cytoplasm H9c2 cardiomyocytes was detected by western blot and normalized to VDAC and GAPDH, respectively; (D,E) H9c2 cardiomyocytes were double stained with Annexin V-FITC and PI-PE, and the apoptosis rate was measured using flow cytometry. The mitochondrial apoptosis pathway was verified by measuring (F) H9c2 cardiomyocyte caspase-3 activity levels. Statistical comparisons were performed using a one-way ANOVA. *, P<0.05 *vs.* control group; #, P<0.05 *vs.* H_2O_2 group; &, P<0.05 *vs.* NAC group. VDAC, voltage-dependent anion channel; GAPDH, glyceraldehyde-3-phosphate dehydrogenase; NAC, N-acetylcysteine; V-FITC, V-fluorescein isothiocyanate; PI, propidium iodide; PE, phycoerythrin; ANOVA, analysis of variance.

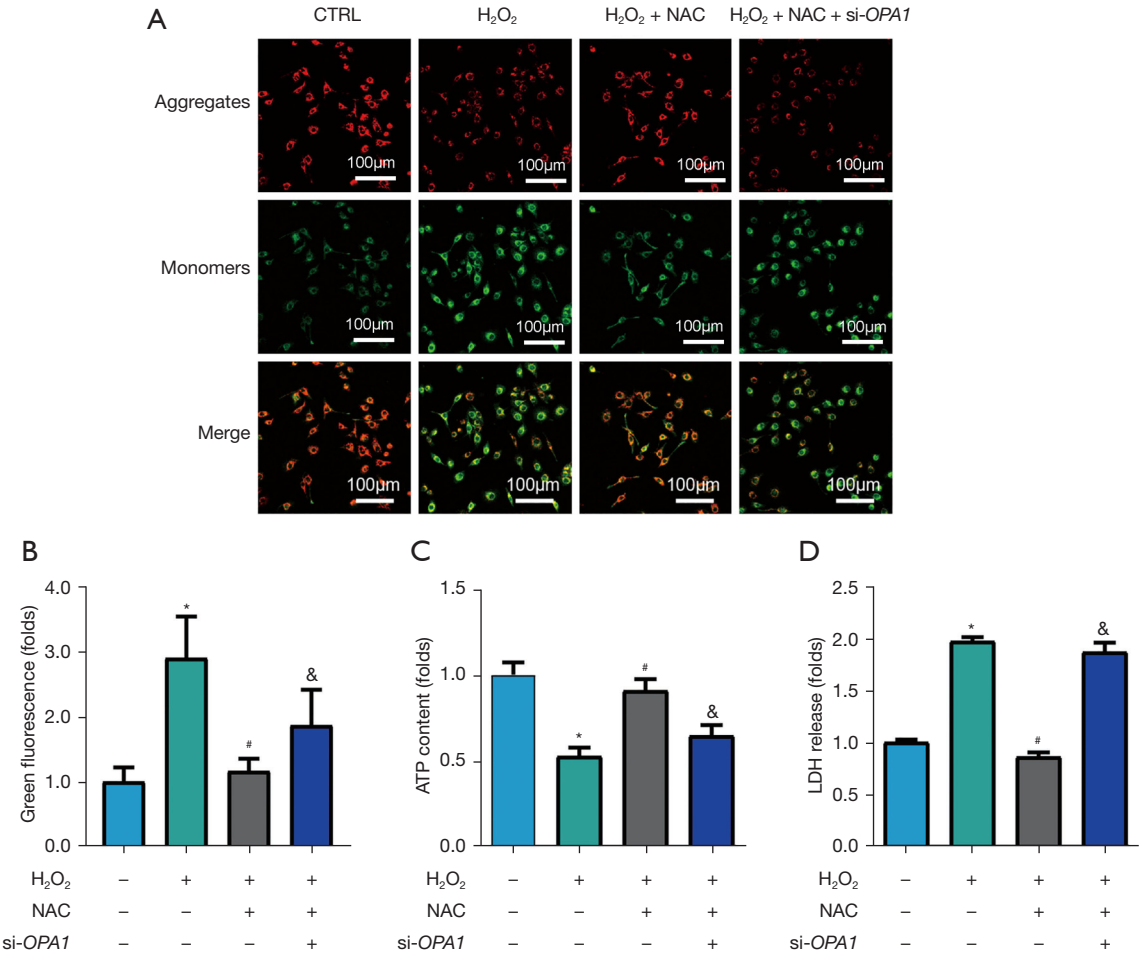

Figure 5 NAC preserves mitochondrial function and structure via *OPA1*. H9c2 cardiomyocytes were treated with 250 μmol/L of H_2O_2 for 12 h with or without 1 mmol/L of NAC pretreatment. Thereafter, (A) the mitochondrial membrane potential assay kit with JC-1 fluorescence probe staining was used to measure ΔΨm in H9c2 cardiomyocytes. (B) Quantification of ΔΨm based on the average fluorescence intensity of monomeric JC-1, which indicates cell depolarization. (C,D) ATP content and LDH production in H9c2 cardiomyocytes were measured to evaluate mitochondrial function. Statistical comparisons were performed using a one-way ANOVA. *, P<0.05 *vs.* control group; #, P<0.05 *vs.* H_2O_2 group; &, P<0.05 *vs.* NAC group. CTRL, control; NAC, N-acetylcysteine; ATP, adenosine triphosphate; LDH, lactate dehydrogenase; ANOVA, analysis of variance.

tissue is associated with the accumulation of dysfunctional mitochondria and heart failure. Using a cardiac lipotoxicity transgenic mouse model and neonatal rat ventricular cardiomyocytes, Tsushima *et al.* (35) observed that lipid overload induced ROS generation and mitochondrial morphological changes, accompanied by the loss of the mitochondrial reticulum and the *OPA1* change. Zhang *et al.* (36) reported that melatonin rectified excessive mitochondrial fission, promoted mitochondria energy metabolism, and reduced cardiomyocyte apoptosis via *OPA1*-related mitochondrial fusion and mitophagy. In the present study, even though we used a different model to induce oxidative stress damage, the changes in mitochondrial morphology and *OPA1* change were consistent with those in previous reports (35,36), indicating that oxidative stress affected mitochondrial fusion. Mitochondrial fusion and fission are usually balanced; decreased fusion is often accompanied by excessive fission. Unlike DRP1, phosphorylation at S616 was observed in Tsushima's (35) experiment. We observed an increase in total DRP1, which was a trigger of fission. These observations suggest that there may be certain differences

in fusion and fission regulation depending on the model employed.

OPA1 can regulate the shape of mitochondrial cristae and maintain their morphology (37). Its downregulation inhibits mitochondrial fusion, triggering fragmentation and cristae remodeling, promoting spontaneous cytochrome c release and apoptosis. Conversely, high *OPA1* expression inhibits cytochrome c release (38,39), protecting cells against apoptosis (40). Therefore, a disbalance in mitochondrial dynamics leads to mitochondrial apoptosis. In the present study, we demonstrated that *OPA1* regulated apoptosis and was involved in the protection of NAC.

While our preliminary study suggests that NAC may alleviate oxidative stress-induced damage in H9c2 cardiomyocytes, it is important to note that there are limitations to our study. MQC is constantly changing, but as we did not observe this process continuously, we might have missed some of the effects of NAC against oxidative stress. Specifically, we did not investigate the effects of NAC on oxidative stress in primary myocardial cells or in animal models. Moving forward, we plan to further investigate the protective effects of NAC on oxidative stress-induced cardiac injury and elucidate the associated molecular mechanisms using doxorubicin and ischemia-reperfusion injury myocardial injury models, as well as mouse primary cardiomyocytes.

Conclusions

Collectively, our results indicated that NAC mitigates the damage of H9c2 cardiomyocytes induced by H_2O_2 via stimulating OPA1, thereby enhancing mitochondrial function and reducing apoptosis. We clarified the cardioprotective effect of NAC from the aspect of MQC and provided a possible theoretical basis for future novel clinical applications of NAC to treat cardiac disease.

Acknowledgments

Funding: This work was supported by the Science and Technology Fund of the Tianjin Health Commission (No. 2015KZ071), and the Tianjin Key Medical Discipline (Specialty) Construction Project (No. TJYXZDXK-055B).

Footnote

Reporting Checklist: The authors have completed the MDAR reporting checklist. Available at https://jtd.amegroups.com/article/view/10.21037/jtd-24-927/rc

Data Sharing Statement: Available at https://jtd.amegroups.com/article/view/10.21037/jtd-24-927/dss

Peer Review File: Available at https://jtd.amegroups.com/article/view/10.21037/jtd-24-927/prf

Conflicts of Interest: All authors have completed the ICMJE uniform disclosure form (available at https://jtd.amegroups.com/article/view/10.21037/jtd-24-927/coif). The authors have no conflicts of interest to declare.

Ethical Statement: The authors are accountable for all aspects of the work in ensuring that questions related to the accuracy or integrity of any part of the work are appropriately investigated and resolved.

References

1. Wan J, Zhang Z, Wu C, et al. Astragaloside IV derivative HHQ16 ameliorates infarction-induced hypertrophy and heart failure through degradation of lncRNA4012/9456. Signal Transduct Target Ther 2023;8:414.
2. Silva-Palacios A, Zazueta C, Pedraza-Chaverri J. ER membranes associated with mitochondria: Possible therapeutic targets in heart-associated diseases. Pharmacol Res 2020;156:104758.
3. Xu H, Yu W, Sun M, et al. Syntaxin17 contributes to obesity cardiomyopathy through promoting mitochondrial Ca(2+) overload in a Parkin-MCUb-dependent manner. Metabolism 2023;143:155551.
4. Kumar AA, Kelly DP, Chirinos JA. Mitochondrial Dysfunction in Heart Failure With Preserved Ejection Fraction. Circulation 2019;139:1435-50.
5. Elorza AA, Soffia JP. mtDNA Heteroplasmy at the Core of Aging-Associated Heart Failure. An Integrative View of OXPHOS and Mitochondrial Life Cycle in

Cardiac Mitochondrial Physiology. Front Cell Dev Biol 2021;9:625020.
6. Lin KL, Chen SD, Lin KJ, et al. Quality Matters? The Involvement of Mitochondrial Quality Control in Cardiovascular Disease. Front Cell Dev Biol 2021;9:636295.
7. Nomura R, Sato T, Sato Y, et al. Azidothymidine-triphosphate impairs mitochondrial dynamics by disrupting the quality control system. Redox Biol 2017;13:407-17.
8. Chen W, Zhao H, Li Y. Mitochondrial dynamics in health and disease: mechanisms and potential targets. Signal Transduct Target Ther 2023;8:333.
9. Haileselassie B, Mukherjee R, Joshi AU, et al. Drp1/Fis1 interaction mediates mitochondrial dysfunction in septic cardiomyopathy. J Mol Cell Cardiol 2019;130:160-9.
10. Gao F, Liang T, Lu YW, et al. Reduced Mitochondrial Protein Translation Promotes Cardiomyocyte Proliferation and Heart Regeneration. Circulation 2023;148:1887-906.
11. Da Dalt L, Cabodevilla AG, Goldberg IJ, et al. Cardiac lipid metabolism, mitochondrial function, and heart failure. Cardiovasc Res 2023;119:1905-14.
12. Hara H, Araya J, Ito S, et al. Mitochondrial fragmentation in cigarette smoke-induced bronchial epithelial cell senescence. Am J Physiol Lung Cell Mol Physiol 2013;305:L737-46.
13. Ishihara N, Fujita Y, Oka T, et al. Regulation of mitochondrial morphology through proteolytic cleavage of OPA1. EMBO J 2006;25:2966-77.
14. Rovira-Llopis S, Bañuls C, Diaz-Morales N, et al. Mitochondrial dynamics in type 2 diabetes: Pathophysiological implications. Redox Biol 2017;11:637-45.
15. Hu C, Shu L, Huang X, et al. OPA1 and MICOS Regulate mitochondrial crista dynamics and formation. Cell Death Dis 2020;11:940.
16. Jian F, Chen D, Chen L, et al. Sam50 Regulates PINK1-Parkin-Mediated Mitophagy by Controlling PINK1 Stability and Mitochondrial Morphology. Cell Rep 2018;23:2989-3005.
17. Li W, Li Y, Siraj S, et al. FUN14 Domain-Containing 1-Mediated Mitophagy Suppresses Hepatocarcinogenesis by Inhibition of Inflammasome Activation in Mice. Hepatology 2019;69:604-21.
18. Wai T, García-Prieto J, Baker MJ, et al. Imbalanced OPA1 processing and mitochondrial fragmentation cause heart failure in mice. Science 2015;350:aad0116.
19. Vásquez-Trincado C, García-Carvajal I, Pennanen C, et al. Mitochondrial dynamics, mitophagy and cardiovascular disease. J Physiol 2016;594:509-25.
20. Patten DA, Wong J, Khacho M, et al. OPA1-dependent cristae modulation is essential for cellular adaptation to metabolic demand. EMBO J 2014;33:2676-91.
21. Gilkerson R, De La Torre P, St Vallier S. Mitochondrial OMA1 and OPA1 as Gatekeepers of Organellar Structure/Function and Cellular Stress Response. Front Cell Dev Biol 2021;9:626117.
22. Sahasrabudhe SA, Terluk MR, Kartha RV. N-acetylcysteine Pharmacology and Applications in Rare Diseases-Repurposing an Old Antioxidant. Antioxidants (Basel) 2023;12:1316.
23. Song G, Wang J, Liu J, et al. Dimethyl fumarate ameliorates erectile dysfunction in bilateral cavernous nerve injury rats by inhibiting oxidative stress and NLRP3 inflammasome-mediated pyroptosis of nerve via activation of Nrf2/HO-1 signaling pathway. Redox Biol 2023;68:102938.
24. Kumar S, Sitasawad SL. N-acetylcysteine prevents glucose/glucose oxidase-induced oxidative stress, mitochondrial damage and apoptosis in H9c2 cells. Life Sci 2009;84:328-36.
25. Yang L, Guan G, Lei L, et al. Oxidative and endoplasmic reticulum stresses are involved in palmitic acid-induced H9c2 cell apoptosis. Biosci Rep 2019;39:BSR20190225.
26. Kuno A, Hosoda R, Tsukamoto M, et al. SIRT1 in the cardiomyocyte counteracts doxorubicin-induced cardiotoxicity via regulating histone H2AX. Cardiovasc Res 2023;118:3360-73.
27. Cao H, Xu H, Zhu G, et al. Isoquercetin ameliorated hypoxia/reoxygenation-induced H9C2 cardiomyocyte apoptosis via a mitochondrial-dependent pathway. Biomed Pharmacother 2017;95:938-43.
28. Xie S, Deng W, Chen J, et al. Andrographolide Protects Against Adverse Cardiac Remodeling After Myocardial Infarction through Enhancing Nrf2 Signaling Pathway. Int J Biol Sci 2020;16:12-26.
29. Popov SV, Mukhomedzyanov AV, Voronkov NS, et al. Regulation of autophagy of the heart in ischemia and reperfusion. Apoptosis 2023;28:55-80.
30. Wang K, Liu F, Zhou LY, et al. miR-874 regulates myocardial necrosis by targeting caspase-8. Cell Death Dis 2013;4:e709.
31. Baechler BL, Bloemberg D, Quadrilatero J. Mitophagy regulates mitochondrial network signaling, oxidative stress, and apoptosis during myoblast differentiation. Autophagy 2019;15:1606-19.
32. Wang JX, Zhang XJ, Li Q, et al. MicroRNA-103/107

Regulate Programmed Necrosis and Myocardial Ischemia/Reperfusion Injury Through Targeting FADD. Circ Res 2015;117:352-63.
33. Wang ZH, Liu JL, Wu L, et al. Concentration-dependent wrestling between detrimental and protective effects of H2O2 during myocardial ischemia/reperfusion. Cell Death Dis 2014;5:e1297.
34. Lin CJ, Lee CC, Shih YL, et al. Resveratrol enhances the therapeutic effect of temozolomide against malignant glioma in vitro and in vivo by inhibiting autophagy. Free Radic Biol Med 2012;52:377-91.
35. Tsushima K, Bugger H, Wende AR, et al. Mitochondrial Reactive Oxygen Species in Lipotoxic Hearts Induce Post-Translational Modifications of AKAP121, DRP1, and OPA1 That Promote Mitochondrial Fission. Circ Res 2018;122:58-73.
36. Zhang Y, Wang Y, Xu J, et al. Melatonin attenuates myocardial ischemia-reperfusion injury via improving mitochondrial fusion/mitophagy and activating the AMPK-OPA1 signaling pathways. J Pineal Res 2019;66:e12542.
37. Frezza C, Cipolat S, Martins de Brito O, et al. OPA1 controls apoptotic cristae remodeling independently from mitochondrial fusion. Cell 2006;126:177-89.
38. Griparic L, van der Wel NN, Orozco IJ, et al. Loss of the intermembrane space protein Mgm1/OPA1 induces swelling and localized constrictions along the lengths of mitochondria. J Biol Chem 2004;279:18792-8.
39. Faccenda D, Nakamura J, Gorini G, et al. Control of Mitochondrial Remodeling by the ATPase Inhibitory Factor 1 Unveils a Pro-survival Relay via OPA1. Cell Rep 2017;18:1869-83.
40. Varanita T, Soriano ME, Romanello V, et al. The OPA1-dependent mitochondrial cristae remodeling pathway controls atrophic, apoptotic, and ischemic tissue damage. Cell Metab 2015;21:834-44.

(English Language Editor: L. Huleatt)

Cite this article as: Zheng J, Zhao L, Liu Y, Chen M, Guo X, Wang J. N-acetylcysteine, a small molecule scavenger of reactive oxygen species, alleviates cardiomyocyte damage by regulating *OPA1*-mediated mitochondrial quality control and apoptosis in response to oxidative stress. J Thorac Dis 2024;16(8):5323-5336. doi: 10.21037/jtd-24-927